Sediment Soot Radiocarbon Indicates that Recent Pollution Controls Slowed Fossil Fuel Emissions in Southeastern China

Han, Yongming; An, Zhisheng; Arimoto, Richard; Waters, Colin N.; Schneider, Tobias; Yao, Peng; Sarli, Eirini; Zhou, Weijian; Li, Li; Dusek, Ulrike

Published in:
Environmental Science and Technology

DOI:
10.1021/acs.est.1c05424

Environmental Science & Technology

pubs.acs.org/est

Article

Sediment Soot Radiocarbon Indicates that Recent Pollution Controls Slowed Fossil Fuel Emissions in Southeastern China

Yongming Han,* Zhisheng An, Richard Arimoto, Colin N. Waters, Tobias Schneider, Peng Yao, Eirini Sarli, Weijian Zhou, Li Li, and Ulrike Dusek*

Cite This: *Environ. Sci. Technol.* 2022, 56, 1534−1543

Read Online

ACCESS | Metrics & More | Article Recommendations | Supporting Information

ABSTRACT: Fossil fuel (FF) combustion emissions account for a large, but uncertain, amount of the soot in the atmosphere, play an important role in climate change, and adversely affect human health. However, historical estimates of FF contributions to air pollution are limited by uncertainties in fuel usage and emission factors. Here, we constrained FF soot emissions from southeastern China over the past 110 years, based on a novel radiocarbon method applied to sedimentary soot. The reconstructed soot accumulations reflect the integrated effects of increased FF use caused by economic development and reductions in emissions due to pollution controls. A sharp increase in FF soot started in 1950 as southeastern China industrialized and developed economically, but decreased FF soot fluxes in recent years suggest that pollution controls reduced soot emissions. We compare FF soot history to changes in CO_2 emissions, industrial and economic activities, and pollution controls and show that FF soot fluxes are more readily controlled than atmospheric CO_2. Our independent FF soot record provides insights into the effects of economic development and controls on air pollution and the environmental impacts from the changes in soot emissions.

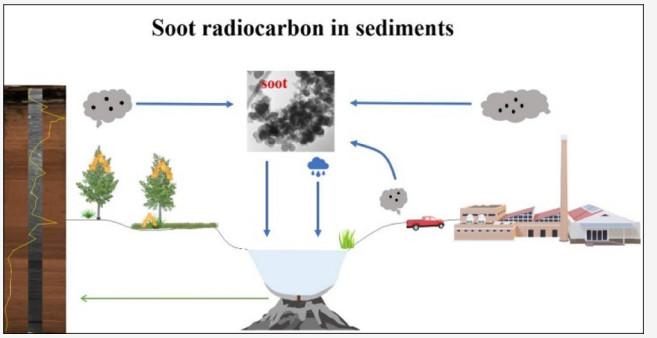

KEYWORDS: *fossil fuel usage, black carbon, human emissions, pollution history, lake sediments*

1. INTRODUCTION

The burning of biomass (BB) and fossil fuels (FFs) has affected the ecology, environment, and climate of the Earth in complex ways. The transition from BB to FF as the main energy source during onset of the industrial interval (post-1850 CE) was a turning point in the evolution of human society[1] that also led to rapid environmental changes, including increased emissions of air pollutants, both greenhouse gases and particulate matter. These emissions have caused growing concerns over their impacts on climate, the environment, and public health.[2] More generally, there have been concerns over the profound shift in the Earth System from its Holocene envelope of natural variability to the proposed current epoch, the Anthropocene, in which human impacts, most notably through FF combustion, have significantly altered Earth System processes.[3,4]

Information on the historical variations in the amounts of BB versus FF in combustion emissions is a key to understanding anthropogenic impacts on the Earth System. Assessments of their environmental impacts in the past decades have mainly focused on reconstructed emission inventories calculated from documented fuel usage and assumed emission factors for pollutants such as CO_2 and black carbon (BC).[5,6] This approach is fraught with uncertainties due to strong geographic differences in degrees of industrialization and the efficiency of energy usage and associated emission factors.

Information on the changes in anthropogenic FF emissions uncovered through analyses of stratigraphic records provides a new approach for studying historical trends in BB versus FF emissions; that is, changes in societal structures, population, and energy usage can be related to their impacts on the environment through records of pollutant deposition reconstructed from sediment accumulations through time.[3] This is particularly valuable for time periods before which instrumental observations of pollution concentrations are available.

BC is composed of refractory carbonaceous particles produced by the incomplete combustion of biomass and FFs.[7,8] It can be regarded as a "combustion continuum" that includes both combustion condensates and residues and contains a mixture of chemical species.[8−10] It can be preserved in various sedimentary environments for more than a million years[11] and thus can be used to evaluate historical variations in

Received: August 12, 2021
Revised: December 17, 2021
Accepted: December 20, 2021
Published: January 10, 2022

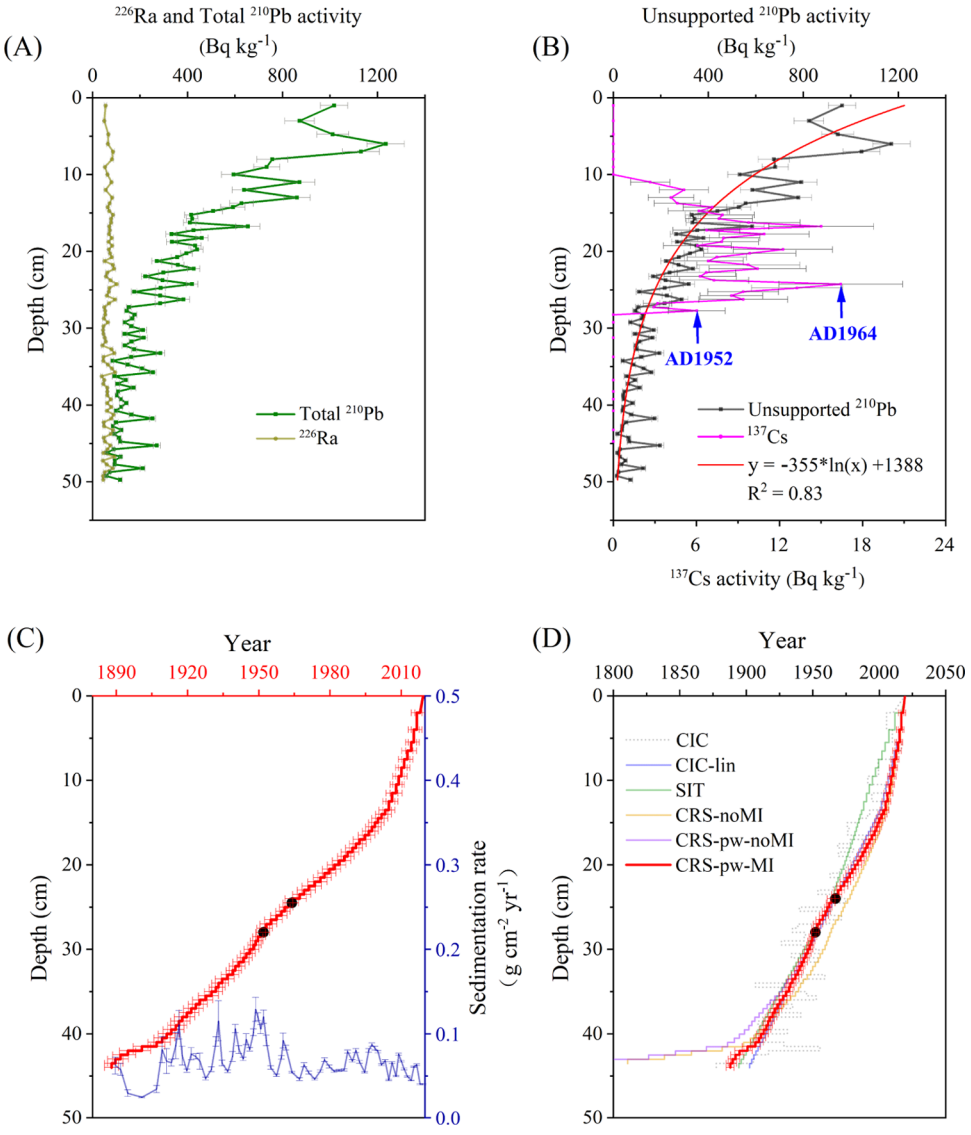

Figure 1. Age-depth model for sediment core of the HGY Lake in southern China. (A) Total ^{210}Pb and ^{226}Ra activities versus depth (with uncertainties), (B) unsupported ^{210}Pb and ^{137}Cs activities versus depth (with uncertainties); the red line shows the logarithmic fitting line of the unsupported ^{210}Pb; arrows highlight the start of global nuclear testing in 1952 and the peak in global nuclear fallout in 1964, (C) chronology reconstruction using the piecewise CRS model (red line with uncertainties) and the calculated sedimentation rates (blue line with uncertainties), and (D) comparison among the different chronology models (see the text and Supporting Information part for detailed explanations of the different models). The black dots in (C,D) highlight the constrained points of the years 1952 (at a depth of 27.75 cm) and 1964 (at a depth of 24.25 cm), respectively. The error bars indicate uncertainties.

combustion emissions. Furthermore, BC can absorb solar radiation in the atmosphere and so contributes to global warming.[7] BC aerosols also can modify precipitation patterns, promote glacial melting, and cause severe harmful effects to human health.[8,9] BC is composed of two carbonaceous subtypes[12] (see Supporting Information, for details), soot (combustion condensates), and char (combustion residues). Soot particles are mainly submicron in size, and because they are smaller than char, they are more easily transported over regional or larger scales.[10] It is thus of great environmental importance to determine the relative amounts of soot produced during FF or biomass combustion and the extent to which this has changed over time.

Radiocarbon (^{14}C) measurements are a robust and independent tool for differentiating BB from FF emissions, and this method has been widely used for apportioning the sources of carbonaceous aerosols, especially organic carbon (OC) and BC.[13−19] Radiocarbon techniques for the analysis of BC in geological materials may also help quantify the FF impacts on the environment and provide a robust marker to help characterize the mid-20th century onset of the Anthropocene Epoch. However, these methods have never been used to determine BC radiocarbon in sediments, and apart from one ice-core radiocarbon record,[20] only emission inventories have been used to assess FF−BC historical trends.[5,6]

BC deposits in the sediments of maar lakes are ideally suited for studies of environmental change on a regional or broader scale because accumulations of exogenic materials in these lakes are almost entirely from atmospheric deposition.[21] In this study, we investigated soot radiocarbon in sediments of Huguangyan Lake (HGY) in southeastern China (see

https://doi.org/10.1021/acs.est.1c05424
Environ. Sci. Technol. 2022, 56, 1534−1543

Supporting Information section S1; Figures S1 and S2). The objectives of the study were (1) to develop an independent, archive-based approach for differentiating the FF fractions of soot (%FF soot) in sediments from the BB fractions (%BB soot), (2) to reconstruct the records of the relative FF fractions in soot and of the soot fluxes from FF versus biomass combustion (BB and FF soot flux), respectively, and (3) to discuss the impacts of economic development and economic and environmental policies on the variations of FF soot fluxes and to highlight the unique insights that can be obtained from archival records compared with fuel usage-based BC emission inventories. The study not only provides a historical perspective on air pollution in southeastern China but also documents human impacts during the Anthropocene.

2. METHODS AND MATERIALS

The HGY Lake (21°8.65′ N, 110°16.81′ E; 23 m asl) is located near Zhanjiang, Guangdong, in southeastern China (Figure S1). The endorheic maar lake has a water surface area of ∼2.3 km^2 and a catchment of ∼3.2 km^2. The circular lake is about 22 m deep, and there are no fluvial inlets or outlets. As a volcanic crater lake, it has a steep outer lava wall, forming a small lake catchment. Thus, the inputs of pollutants and other materials to the lake are almost exclusively from atmospheric deposition, and the local contributions would be very small. The region is impacted by the East Asia monsoon, and the precipitation is concentrated during summer, averaging at 1600 mm per year.

Four cores were collected in parallel using a gravity corer in the depocenter (21 m water depth) of HGY Lake (Figures S1 and S2) in April, 2019 (see Supporting Information section S1 for details). The ^{210}Pb, ^{137}Cs, and ^{226}Ra activities were measured to establish the sediment chronology. We calculated three different age-depth models (CIC: constant initial concentration, CRS: constant rate of supply, and SIT: sediment isotope tomography) with and without missing inventory correction[22] to assess the robustness of the chronologies (see Supporting Information section S2 for details). The ^{137}Cs activities were used as an independent chrono-marker to constrain the chronologies at 24.25 cm depth to 1964 CE (nuclear weapon test fallout peak) and at 27.75 cm depth to 1952 CE (^{137}Cs-fallout onset) (Figure 1B). The mass accumulation rates (MAR, g cm^{-2} yr^{-1}) (Figure 1C) were derived from the age-depth models and used to calculate compound fluxes (BC, soot, and char). Additional details concerning the chronology and age-depth modeling may be found in Supporting Information section S2.

BC, char, and soot concentrations were measured using a thermal/optical method following previous publications[12,23] (see Supporting Information section S3 for details). In this study, we developed a method for separating soot from OC and char that made use of a newly developed automated aerosol combustion system,[24] as explained in detail in Supporting Information section S4. A series of tests (Figures S6−S9) were conducted to optimize the method used to isolate the refractory soot fraction. Several char and soot standard reference materials (see Supporting Information section S4 and S5, Figure S10, Table S1) were tested and showed that only a few percent of the char remained. Then, radiocarbon analysis of isolated soot was performed using the gas inlet system[25] of the mini carbon dating system accelerator mass spectrometer (AMS)[26] at the Center for Isotope Research in the Energy and Sustainability Research Institute Groningen, the Netherlands.

The radiocarbon values are reported as the "fraction modern" ($F^{14}C$) defined by Reimer et al.[27]

$$F^{14}C = \frac{(^{14}C/^{12}C)_{sample,\,[-25]}}{0.7459 \times (^{14}C/^{12}C)_{OXII,\,[-25]}} \quad (1)$$

where the $^{14}C/^{12}C$ ratio of a sample is reported relative to that of an oxalic acid standard (OXII) and both ratios are normalized to $\delta^{13}C = -25‰$. The $F^{14}C$ values were corrected for memory effects and instrument background,[28] and they were normalized to the average value (memory- and background-corrected) of gaseous OXII standards—that corrected for any contamination introduced during the AMS measurements. The average soot recovery for radiocarbon analysis of the samples from HGY Lake was 93 ± 24% (compared against soot values measured by thermal−optical analysis). Details for isolation of soot, radiocarbon analyses, and quality control can be found in Supporting Information section S4. Finally, uncertainty estimates of compound (BC, soot, char, FF soot, and BB soot) fluxes were calculated by propagating the uncertainties of three factors, including compound concentrations, MARs, and FF fraction calculations (see Supporting Information section S6 for details).

3. RESULTS AND DISCUSSION

3.1. Chronological Control. The sediment chronology is based on high-resolution (0.5 cm) radionuclide dating (^{226}Ra, ^{210}Pb, and ^{137}Cs) (Figure 1). Except for a slight deviation toward the surface, the unsupported ^{210}Pb ($^{210}Pb_{un.}$) activities in the HGY Lake sediments showed an exponential decrease with depth (Figure 1B). Careful examination of the ^{137}Cs profile enabled identification of the following two specific chrono-marker depths (Figure 1B): (i) the onset of the ^{137}Cs fallout (year 1952 CE) at 27.75 cm sediment depth and (ii) the nuclear weapon fallout peak (year 1964 CE) at 24.25 cm.

The comparison of different age-depth models (CIC, SIT, and CRS; Figure 1D) shows that the piecewise-constant rate of the supply model (CRS-pw-MI, Figure 1C; see Supporting Information section S2), constrained with the independent ^{137}Cs chrono-markers for 1964 CE and 1952 CE[29] and a missing inventory correction,[22] produced the most reliable results. The CRS-pw-MI results (Figure 1C) are comparable with those of previous studies,[23,30] and thus, this age-depth model was selected for compound flux calculations (BC, char, and soot). Constraining the CRS model with the independent chrono-markers produced very small age uncertainties (red line with uncertainties in Figure 1C), from maximum values of ±2.9 years (two sigma) for the post-1950 period to the maximum uncertainties of ±3.7 years (two sigma) for the period of ∼1950−1887, with the largest uncertainties observed toward the bottom of the profile (more details in Supporting Information section S2).

3.2. Rapid Increase in FF Fractions of Soot Since 1950 and Its Causes. The measured $F^{14}C$ values of soot in HGY Lake sediments were relatively stable from 1910 to the late 1940s, and subsequently, they sharply decreased and began fluctuating (Figure 2B). The rapid decrease in $F^{14}C$ starting in ∼1950 may have been impacted to a degree by global nuclear weapon tests. Measurements of BC $F^{14}C$ in fine particulate matter ($PM_{2.5}$, aerodynamic diameter ≤2.5 μm) in Hainan Province, which is very close to the study location, show that

https://doi.org/10.1021/acs.est.1c05424
Environ. Sci. Technol. 2022, 56, 1534−1543

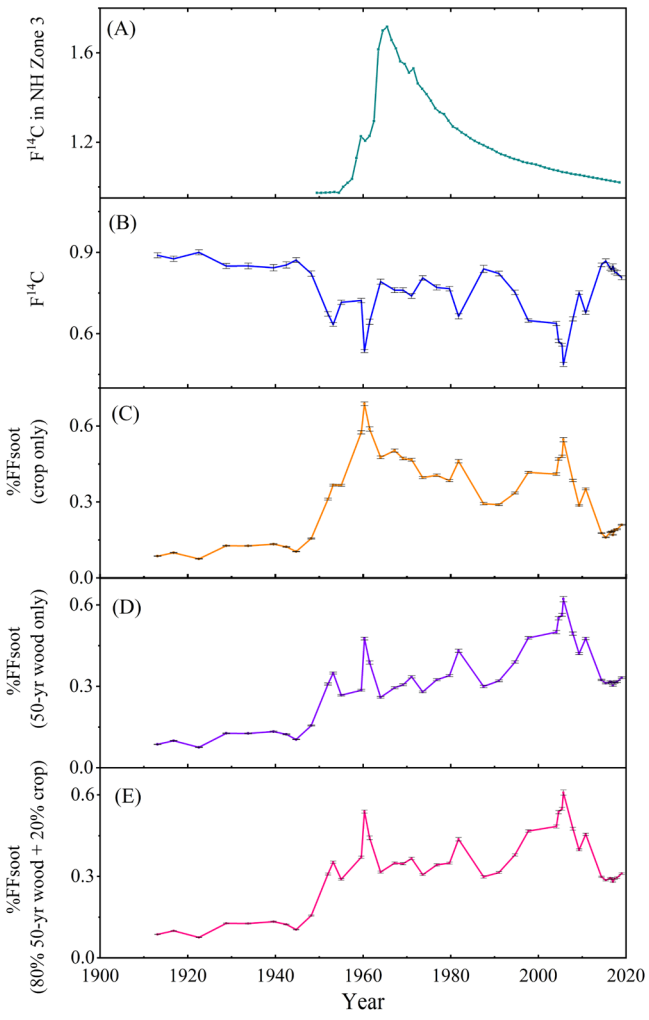

Figure 2. Measured fraction modern ($F^{14}C$, see text) values and the calculated %FF soot for sediments from HGY Lake. (A) $F^{14}C$ values in Northern Hemisphere zone 3 used in this study for corrections, (B) measured $F^{14}C$ values (with uncertainties; gray bars) in HGY Lake, (C–D) calculated %FF soot for the assumption of crops only and wood only (we assume 50 yr old wood with exponential growth), respectively, and (E) %FF soot calculated for the assumption of 80% wood (50 yr with exponential growth) and 20% crops.[32] Note: uncertainties in (B–E) presented in gray bars only indicate those from the $F^{14}C$ measurement uncertainties.

$F^{14}C$ values can vary depending on meteorology and air mass history.[31] The average $F^{14}C$ of airborne BC in the study in the year 2005/06 was 0.69 ± 0.13, which agrees well with the $F^{14}C$ value of 0.65 of the soot recovered from sediments at the same time in this study (Figure 2B).

The %FF soot in the sediments is calculated (Figure 2) by considering four factors: (1) The study location in the Northern Hemisphere zone 3 (http://calib.org/CALIBomb/), (2) variability in the relative contributions of BC emissions from wood versus crop combustion,[32] (3) age of the wood burned, and (4) how the wood that was burned grew. We assume for the %FF soot calculation that the materials burned were a mixture of 80% wood and 20% crops and that the wood was 50 y old and came from trees that had exponential growth (Supporting Information section S5 explains the reasons for these assumptions). The overall %FF soot uncertainty was calculated to be 0.08–21.0% and averaged 7.5%.

The %FF soot (Figure 3A) showed low values and a slowly increasing trend (ranging from 7.5–13.3% and averaging 10.9%) from the 1910s to the 1940s, followed by a rapid increase starting in 1950. Thereafter, the %FF soot fluctuated over higher values, between 28.05 and 60.8%, and prominent peaks were evident in 1953, 1960, and 1981. The highest %FF soot was in 2005, and after that, there was an overall decrease, a small peak at 2011, and finally, a sharp decrease to relatively stable values from 28.6 to 31.0%.

The relatively low %FF soot before 1950 (Figure 3A) can be regarded as an indicator of the state of the atmosphere prior to the pre-modern industrialization of China. The initial industrialization, which occurred in southern and eastern China, can be traced back to the Westernization Movement during the Qing Dynasty in the 1870s. The abrupt increase in %FF soot in 1950 (Figure 3A) corresponds with the establishment of the People's Republic of China (PRC). This excursion can be considered a marker for the beginning of the modern industrialization of China, and it reflects a major shift in energy usage, from low efficient BB (with an initial post-1950 decrease in BB soot flux, Figure 3E) to more efficient FF (with an initial post-1950 increase in FF soot flux, Figure 3B).

Previous studies have shown that variations in char/soot ratios provide insights into the relative contributions of BB versus FF to the loadings of carbonaceous aerosols.[10] A decrease in the char/soot ratio from >4.0 in the 1940s to < ~3.0 in the early 1950s and an overall decreasing trend in char/soot ratios from older to younger sediments (Figure S4D) support the idea that the proportions of the two BC subtypes changed when FFs were increasingly used for industrial and transport purposes. Even so, the char/soot ratio does not give quantitative information on the contributions from BB versus FF because combustion conditions, especially whether the fires are flaming or smoldering, also affect the relative amounts of char and soot in the emissions.[11]

The first major peak for the %FF soot (53.9%) was found during 1960–1961 (Figure 3A) that followed the "three years of natural disasters" from 1958 to 1960, when China promoted industrial development (Figure 3C) and de-emphasized agricultural production (Figure 3F). The first national "economic adjustment" started in 1961, and its objective was to reduce the focus on industrial activities in favor of agricultural production.[33] The largest %FF soot peak (60.9%) we observed occurred in 2005, which is when the national emission standards for coal-fired power plants were put into place.[34] The main intent of this action was to decrease the quantities of sulfur emitted from coal-fired power plants, and the regulations did in fact cause a substantial decrease in atmospheric sulfate after 2006.[35] However, coal-fired power plants are also a well-known source for BC, and we demonstrate here that the implementation of the regulations is synchronous with a clear decrease in %FF soot at the rural HGY receptor site in southeastern China (Figure 3A) despite an increase in energy usage at the same time (Figure 3D).

Problems with aerosol pollution were an unfortunate consequence of the rapid industrial and economic development in China. In 2012, national emission standards for coal-fired power plants[34,35] were introduced to reduce the loadings of $PM_{2.5}$. These control measures resulted in a reduction of the national population–weighted annual mean $PM_{2.5}$ mass concentrations from 61.8 to 42.0 $\mu g\ m^{-3}$ from 2013 to

https://doi.org/10.1021/acs.est.1c05424
Environ. Sci. Technol. 2022, 56, 1534–1543

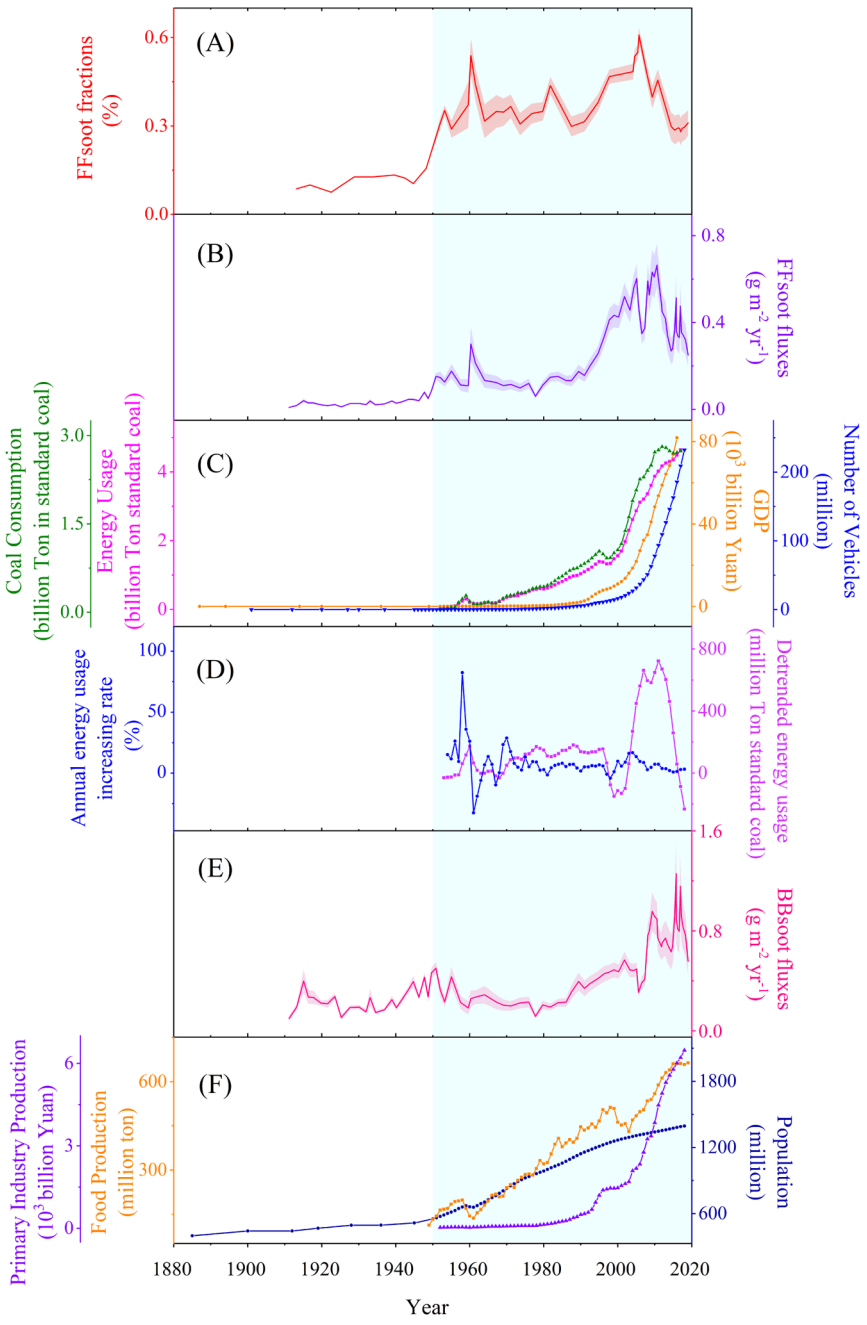

Figure 3. Historical soot fluxes separated into BB and FF sources versus statistical economic data. (A) Calculated FF fractions of soot fluxes under the assumption of 80% wood (50 yr with exponential growth) and 20% crops, (B) FF soot fluxes, (C) data for GDP, energy usage, coal consumption, and numbers of motor vehicles in China, (D) annual energy usage rates of increase and detrended energy usage, (E) BB soot fluxes, and (F) data for population, primary industry production, and food production in China. Economic, industrial, and agricultural data since 1950 are from National Bureau of Statistics of China (http://data.stats.gov.cn/easyquery.htm?cn=C01&zb=A0G0I&sj=2018). For the data before 1950, the population is from ref 43, vehicle numbers from ref 44, coal consumption from ref 45 and GDP from ref 46. The shadowed areas in pale turquoise highlight the post-1950 period. Annual energy usage increasing rates in figure B are calculated using the amount of energy usage in a specific year divided by the previous-year value; the detrended energy usages are calculated using the original energy usage minus the energy usage after the exponential regression (Figure S5). Note: the shadowed areas in (A,B,E) indicate the uncertainties; uncertainties of FF soot fractions in (A) include both from $F^{14}C$ measurement and from estimation of the ratio of crop versus tree and the age of the trees that were burned, which are described in the text and Supporting Information section S4.

2017.[35] During this period, the government also introduced measures to reduce industrial emissions, upgrade industrial boilers, and so on,[35] and the decreases in the %FF soot we observed after 2011 (Figure 3A) were likely a consequence of these controls. In addition, in some regions, especially rural areas of northern China, bans on small combustion boilers caused a return to the use of biomass for residential heating with resulting increases in BB soot fluxes (Figure 3E), and that also may have affected the %FF soot values.

3.3. Changes in BB and FF Contributions to Soot Fluxes Related to Anthropogenic Emissions. Overall, the concentrations and fluxes of BC, char, and soot exhibited

https://doi.org/10.1021/acs.est.1c05424
Environ. Sci. Technol. 2022, 56, 1534−1543

increasing trends from older to younger sediments (Figure S4), especially after 1990. There were two rapid periods of increase for all three of these species, one around 1911 and the other in 1950; these correspond with the establishment of the Republic of China and the People's Republic of China (PRC), respectively. The accelerating increase after 1990 has persisted until today, and high concentrations and fluxes can be seen from 2000 to present. This post-2000 interval closely corresponds with the rapid increases in the gross domestic production (GDP) and energy usage of China (Figure 3C) and primary industry production (Figure 3F).

We further separated the soot fluxes into FF and BB contributions (Figure 3B,E) based on the %FF soot and %BB soot; both showed clearly increasing trends and greater fluctuations in recent decades. Similar to the variations in % FF soot, the FF soot fluxes were at relatively low levels before 1950 (0.01−0.04 g m^{-2} yr^{-1}) but very rapidly (~2.5-fold) increased after 1950 (Figure 3B), following the establishment of PRC. A major peak in FF soot fluxes in 1960 (Figure 3B) corresponded with a large peak in the FF fraction of soot (Figure 3A), and then, the FF soot fluxes decreased sharply due to the first national "economic adjustment".[33]

The 1960 peak in FF soot fluxes (Figure 3B) was not evident in the time series graphs of GDP, energy usage, or coal consumption (Figure 3C) because the exponential growth of these economic indicators (Figure S5) obscured their variations over shorter time periods. Thus, we processed the energy usage data to calculate the annual rates of increase and detrended energy usage variations (Figure 3D). We observed that the annual increasing rates of energy usage and the detrended energy usage both showed major peaks around 1960.

From 1950 to 1990, except for the 1960−1961 peak, the FF soot fluxes were at relatively stable, moderate levels (Figure 3B), which is in agreement with the relatively low GDP and low numbers of vehicles in use during this period (Figure 3C). Furthermore, this period saw the establishment of the People's Commune between 1958 and 1983. The People's Commune in the Mao years had a policy requiring people in some rural villages to prepare meals and eat together, and the implementation of this policy in some regions likely reduced bulk coal burning in China.[33]

Similar to the total soot fluxes (Figure 4A), FF soot fluxes also showed an accelerating increase since 1990, when the GDP and energy usage, including coal consumption, all increased abruptly (Figure 3C). The highest peak of FF soot fluxes was observed in 2010, corresponding to the peak in detrended energy usage (Figure 3D). However, there were two dips that occurred from 2006−07 and 2011−15 (Figure 4A), which corresponded with the implementation of the national emission standards for coal-fired power plants. The first of these standards was issued in 2005 and the more restrictive ones in 2012.[35]

Motor vehicles emit more soot than char,[10] but the FF soot fluxes to the lake sediments (Figure 3B) did not track the increase in the number of vehicles used in China (Figure 3C). A rapid increase in motor vehicle numbers began around 2000 and has continued until today, but the FF soot fluxes increased well before then and have been on a general decreasing trend since 2011. The implementation of increasingly restrictive emission standards for motor vehicles in China must have affected the quantities of soot and other pollutants emitted per vehicle. From the late 1990s to present, the standards for

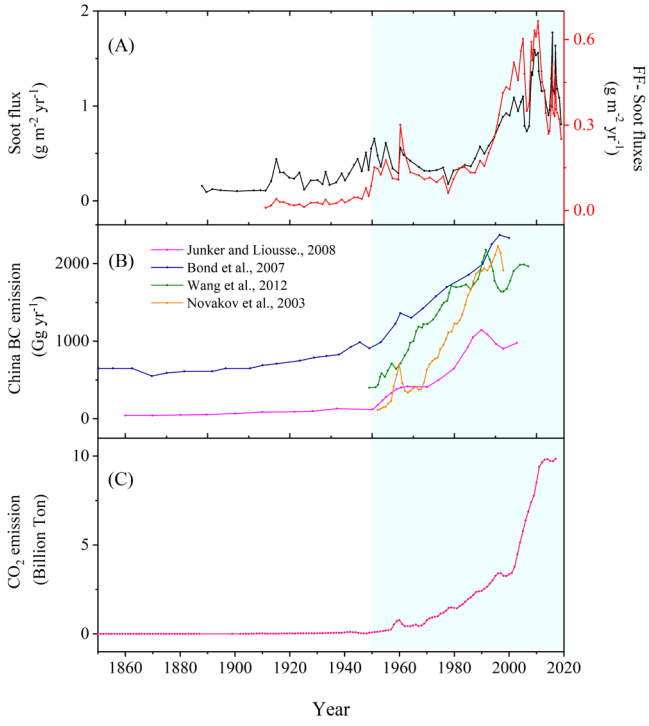

Figure 4. Comparison of historical variations of (A) soot fluxes (black line) and FF soot fluxes (red line) to sediments of the HGY Lake with (C) BC emissions estimated from energy usage[5,6,38,39] and (D) FF CO_2 emissions (data from https://ourworldindata.org/co2-and-other-greenhouse-gas-emissions) in China. The shadowed areas in pale turquoise highlight the post-1950 period.

motor vehicle emissions have evolved from the national standard I to VI—these correspond to the European standards I to VI.

Differences were evident in the reconstructed BB versus FF soot fluxes to the sediments (Figure 3B,E). For example, the BB soot fluxes fluctuated between 1910 and 1990, with a no clear increasing trend, while the FF soot fluxes showed a long-term increase after 1950. From 1945 to 1955, there was a relatively moderate elevation in BB soot fluxes, but no rapid increase. At this time, there were no substantial changes in the production of the primary industries (Figure 3F), which are the ones that use natural raw materials to produce products or industrial materials. Firewood and the burning of domestic and in-field agriculture straw waste are the main sources of BC emissions from BB in China,[32] but the BB soot fluxes appear to have been largely unchanged during the increase in population of the PRC post-1950 (Figure 3E,F). This differs markedly from the conclusion made in a previous study— BB-associated BC emissions increased with population.[32]

Indeed, from 1950 to 1980, there was an overall decrease in BB soot fluxes, with an especially rapid decrease in the mid- to late 1950s (Figure 3E). This was during the People's Commune period, when BC emissions from cooking might have decreased. A rapid increase in BB soot fluxes occurred from the mid-1980s, when primary industrial production started to rise, and has continued to increase to the present (Figure 3F). Similar to FF soot fluxes, BB soot fluxes also exhibited two dips, the first from 2005 to 2006 and the second 2012−2015. This implies that the clean air actions, including those designed to reduce sulfate emissions from coal combustion,[34] also diminished BB emissions.

https://doi.org/10.1021/acs.est.1c05424
Environ. Sci. Technol. 2022, 56, 1534−1543

The low BB soot fluxes from 2005 to 2006 immediately followed a short phase of decreased food production from 2000 to 2004. Straw from food crops including rice, corn, and so on was used for cooking and heating in rural areas. The highest BB soot fluxes were found from 2015−2016, which was likely a consequence of the increasingly restrictive air pollution control measures put in place in 2012.[35] These regulations mainly targeted industrial FF emissions and less attention was given to BB emissions.[35] An upsurge in BB usage in some rural areas for winter heating, especially in parts of northern China, may have increased BB soot during this period.

Previous studies reported that emissions from southeastern and southern Asia forest fires and agricultural burning may also have influenced air pollution in coastal areas of southeastern China.[36] However, the impacts of these influences remain unknown because there is, to our knowledge, no long-term record of BB emissions for southeast Asia. In addition, meteorological factors likely complicate the interpretation of the BB soot deposition results. It is clear, however, that BB plumes from southeastern Asia that pass over the South China Sea would be subject to dispersion and removal processes that would decrease the amount of soot arriving in the HGY region and limit the impact compared with sources from southeastern China (Figure S2). In addition, variations in climate and weather are other important factors influencing local air pollution[37] and thus would affect the soot fluxes to HGY Lake. However, it is beyond the scope of this study to clarify these impacts.

4. IMPLICATIONS FOR AIR POLLUTION CONTROL AND THE ANTHROPOCENE

We developed a novel method for radiocarbon analyses of soot in sediments and applied this method to investigate historical changes in FF and BB soot fluxes as recorded in sediments from a maar lake in southeastern China. We found that the historical soot FF fractions and the FF and BB soot fluxes varied in ways that can be related to changes in economic development, especially industrial and agricultural activities, in China. This suggests that the soot ^{14}C methodology, coupled with high-resolution chronological techniques, enables an independent, archive-based approach for measuring the relative amounts of FF and biomass burned on regional scales.

We note that there are significant discrepancies between our soot and FF soot fluxes compared with the BC emissions reconstructed from statistical records of fuel usage and assumed emission factors[5,6,38,39] (Figure 4). For example, from the mid-1950s to the mid-1980s, our soot and FF soot fluxes showed no pronounced increases but instead were at relatively constant values (Figure 4A), and this is also true for the BB soot fluxes (Figure 3E). In addition to potential impacts from climate and weather, some of the stability in soot and FF soot fluxes during this period may be explained by reductions in cooking emissions associated with the collectivization of meals in the People's Commune from 1958 to 1983. We note that this factor may have been overlooked in the reconstruction of BC emission inventories as rapid and continuous increases in BC emissions were reported for all previous BC inventory reconstructions from the 1950s to at least the end of the millennium[5,6] (Figure 4B). We suggest that cross-verification of fuel usage-based emission inventories with archive-based measurements will lead to more robust estimates of the emissions.

We note that the variations in previous BC emission inventories based on fuel usage[5,6,38,39] resemble those reported for the FF CO_2 emission inventory (Figure 4C), that is, both types of emission inventories showed continuous increases since the mid-1950s but with a pause in the increases in the late 1990s. As there were no specific actions that directly targeted greenhouse gases, the temporal patterns in CO_2 emissions were mainly driven by fuel usage (Figures 3C and 4C). From the 1910s to 2019, the FF CO_2 emissions increased >900 times in China (Figure 4C), while the highest FF soot fluxes (0.665 g m^{-2} yr^{-1} at 2010) were only about 37 times higher than the lowest fluxes (0.012 g m^{-2} yr^{-1} at 1925) during the studied period (Figure 3B).

The large difference between the FF CO_2 emissions and FF soot fluxes can be attributed, at least in part, to the effectiveness of the controls on particulate emissions. For example, closures of small, polluting, and outdated factories began in 2011 and controls also have been placed on industrial emissions, including dust reduction, desulfurization, and denitrification.[34,35] These measures can explain the observed sharp decrease in $PM_{2.5}$ and soot in the atmosphere over the past decade.[34]

Reducing BC emissions has been suggested as a way to combat global warming,[40] and our results show that FF soot fluxes have been much more sensitive to pollution controls than atmospheric CO_2. CO_2 concentrations have been relatively stable after 2011, while FF soot decreased sharply (Figure 4A, C). One of the main reasons for this is that BC has a relatively short atmospheric lifetime compared with CO_2, and another is that there are quantitative differences between the sources for BC and CO_2. The practical implication of these two considerations is that reducing FF emissions will have a more immediate impact on BC than on CO_2 in terms of global warming.

The FF fraction in soot from the lake sediments clearly reflects changes in anthropogenic activities related to economic development in southeastern China and provides information regarding the scale and timing of past air pollution emissions and the implementation of emission controls. For example, the clean air actions since 2005[35] led to lower soot loadings in the atmosphere and lower FF soot fluxes from 2005−2006 (Figure 3B). However, other economic policies, for example, the collectivization of meals for the People's Commune may have contributed to the decrease in soot loadings during the mid-1950s to mid-1980s, even though this would not necessarily be expected. There was another case of a policy that may have contributed to the sharp increase in soot and FF soot fluxes between 1960−1961 (Figure 4A); this was the "Great Leap Forward" during 1958−1959, when China sought to rapidly increase its steel production while focusing less on its agricultural development.[33] These relationships demonstrate that economic and environmental policies targeting air pollution need to take into account the living and economic conditions of the local people.

The transition from BB to FF as the dominant energy source led to technological advances due to the higher energy content of FF, and this change can be used as an indicator of the onset of Anthropocene.[1,3] The transition to FF usage was a milestone in human evolution because of its many important consequences for both human society and the environment. Our study shows that the %FF soot in sediments of HGY Lake increased rapidly in 1950 (Figure 3A), and this year also was the beginning of a "Great Acceleration" in socio-economic and

https://doi.org/10.1021/acs.est.1c05424
Environ. Sci. Technol. 2022, 56, 1534−1543

biophysical systems that transcended climate change.[41] Our results support the mid-20th century as the preferred beginning of the Anthropocene Epoch,[3,42] and we suggest that %FF soot may be a useful marker for the regional correlation of the base of the Anthropocene. As a marker for FF usage, we suggest that our reconstructed record of the FF soot fluxes provides a unique resource for characterizing the Anthropocene. Moreover, the sediment FF data have direct sample-to-sample comparability with environmental and climate proxies in the geological archives, and therefore, our FF soot record provides a means for evaluating the extent to which human FF usage contributed to the expression of the geological Anthropocene in China.

■ ASSOCIATED CONTENT

Supporting Information

The Supporting Information is available free of charge at https://pubs.acs.org/doi/10.1021/acs.est.1c05424.

Site location and sampling; ^{210}Pb, ^{226}Ra, and ^{137}Cs measurements and age-depth modeling; quantification of BC, char, and soot concentrations; extraction and measurement of soot radiocarbon fraction; calculation of FF fractions and their uncertainties; uncertainty estimates of compound fluxes; location of HGY Lake; air mass trajectories; uncertainty estimates for the calculations of FF fractions of soot; fluxes and concentrations of BC, soot, and char, and char/soot ratios; energy usage data; pretreatment assessments and tests for the separation of soot from other carbon fractions; and analyses of standard reference materials with the sediment−soot isolation extraction method (PDF)

■ AUTHOR INFORMATION

Corresponding Authors

Yongming Han − *SKLLQG, Center for Excellence in Quaternary Science and Global Change, Institute of Earth Environment and Center for Excellence in Quaternary Science and Global Change, Chinese Academy of Sciences, Xi'an 710061, China; School of Human Settlements and Civil Engineering, Xi'an Jiaotong University, Xi'an 710049, China;* orcid.org/0000-0002-1282-1354; Phone: number: +86-29-62336276; Email: yongming@ieecas.cn; Fax: +86-29-62336234

Ulrike Dusek − *Centre for Isotope Research (CIO), Energy and Sustainability Research Institute Groningen (ESRIG), Groningen 9747 AG, the Netherlands*; Email: u.dusek@rug.nl

Authors

Zhisheng An − *SKLLQG, Center for Excellence in Quaternary Science and Global Change, Institute of Earth Environment, Chinese Academy of Sciences, Xi'an 710061, China*

Richard Arimoto − *SKLLQG, Center for Excellence in Quaternary Science and Global Change, Institute of Earth Environment, Chinese Academy of Sciences, Xi'an 710061, China*

Colin N. Waters − *School of Geography, Geology and the Environment, University of Leicester, Leicester LE1 7RH, U.K.*

Tobias Schneider − *Department of Geosciences, Morrill Science Center, University of Massachusetts, Amherst, Massachusetts 01003, United States; Lamont-Doherty Earth Observatory of Columbia University, Palisades, New York 10964, United States*

Peng Yao − *Centre for Isotope Research (CIO), Energy and Sustainability Research Institute Groningen (ESRIG), Groningen 9747 AG, the Netherlands;* orcid.org/0000-0002-1265-7849

Eirini Sarli − *Centre for Isotope Research (CIO), Energy and Sustainability Research Institute Groningen (ESRIG), Groningen 9747 AG, the Netherlands*

Weijian Zhou − *SKLLQG, Center for Excellence in Quaternary Science and Global Change, Institute of Earth Environment, Chinese Academy of Sciences, Xi'an 710061, China;* orcid.org/0000-0001-9641-5734

Li Li − *SKLLQG, Center for Excellence in Quaternary Science and Global Change, Institute of Earth Environment, Chinese Academy of Sciences, Xi'an 710061, China*

Complete contact information is available at: https://pubs.acs.org/10.1021/acs.est.1c05424

Author Contributions

Y.H., U.D., and Z.A. designed the study. U.D., Y.H., P.Y., and E.S. performed the analysis. Y.H. and U.D. analyzed the data. T.S. and Y.H. did the chronological dating. Y.H., U.D., R.A., T.S., and C.W. wrote the paper. Y.H., U.D., C.W., R.A., W.Z., T.S., L.L., and Z.A. edited and revised the paper. All authors reviewed and commented on the paper.

Notes

The authors declare no competing financial interest.

■ ACKNOWLEDGMENTS

We thank Lei Dewen and Dr. Lan Jianghu for their field work and Xin Xu for her help in producing the TOC graphic. The constructive comments and suggestions from the three anonymous reviewers are gratefully acknowledged. Also, we are grateful to the HGY Scenic Spot Management Bureau for their support during the fieldwork. This study was supported by the NSFC (41625015 and 41991250), the Strategic Priority Research Program of Chinese Academy of Sciences (XDB40000000), and the Chinese Academy of Sciences (132B61KYSB20170005). T.S. was supported by SNSF early Postdoc. Mobility fellowship # 184428. P.Y. acknowledges the program of China Scholarships Council no. 201806320346.

■ REFERENCES

(1) Syvitski, J.; Waters, C. N.; Day, J.; Milliman, J. D.; Summerhayes, C.; Steffen, W.; Zalasiewicz, J.; Cearreta, A.; Gałuszka, A.; Hajdas, I.; Head, M. J.; Leinfelder, R.; McNeill, J. R.; Poirier, C.; Rose, N. L.; Shotyk, W.; Wagreich, M.; Williams, M. Extraordinary human energy consumption and resultant geological impacts beginning around 1950 CE initiated the proposed Anthropocene Epoch. *Commun. Earth Environ.* **2020**, *1*, 32.

(2) Cifuentes, L.; Borja-Aburto, V. H.; Gouveia, N.; Thurston, G.; Davis, D. L. Hidden Health Benefits of Greenhouse Gas Mitigation. *Science* **2001**, *293*, 1257−1259.

(3) Waters, C. N.; Zalasiewicz, J.; Summerhayes, C.; Barnosky, A. D.; Poirier, C.; Gałuszka, A.; Cearreta, A.; Edgeworth, M.; Ellis, E. C.; Ellis, M.; Jeandel, C.; Leinfelder, R.; McNeill, J. R.; Richter, D. d.; Steffen, W.; Syvitski, J.; Vidas, D.; Wagreich, M.; Williams, M.; An, Z.; Grinevald, J.; Odada, E.; Oreskes, N.; Wolfe, A. P. The Anthropocene is functionally and stratigraphically distinct from the Holocene. *Science* **2016**, *351*, aad2622.

(4) Steffen, W.; Leinfelder, R.; Zalasiewicz, J.; Waters, C. N.; Williams, M.; Summerhayes, C.; Barnosky, A. D.; Cearreta, A.;

Crutzen, P.; Edgeworth, M.; Ellis, E. C.; Fairchild, I. J.; Gałuszka, A.; Grinevald, J.; Haywood, A.; Ivar do Sul, J.; Jeandel, C.; McNeill, J. R.; Odada, E.; Oreskes, N.; Revkin, A.; Richter, D. d.; Syvitski, J.; Vidas, D.; Wagreich, M.; Wing, S. L.; Wolfe, A. P.; Schellnhuber, H. J. Stratigraphic and Earth System approaches to defining the Anthropocene. *Earth's Future* **2016**, *4*, 324−345.

(5) Bond, T. C.; Bhardwaj, E.; Dong, R.; Jogani, R.; Jung, S. K.; Roden, C.; Streets, D. G.; Trautmann, N. M. Historical emissions of black and organic carbon aerosol from energy-related combustion, 1850-2000. *Global Biogeochem. Cycles* **2007**, *21*, GB2018.

(6) Novakov, T.; Ramanathan, V.; Hansen, J. E.; Kirchstetter, T. W.; Sato, M.; Sinton, J. E.; Sathaye, J. A. Large historical changes of fossil-fuel black carbon aerosols. *Geophys. Res. Lett.* **2003**, *30*, 1324.

(7) Ramanathan, V.; Carmichael, G. Global and regional climate changes due to black carbon. *Nat. Geosci.* **2008**, *1*, 221−227.

(8) Masiello, C. A. New directions in black carbon organic geochemistry. *Mar. Chem.* **2004**, *92*, 201−213.

(9) Janssen, N. A.; Gerlofs-Nijland, M. E.; Lanki, T.; Salonen, R. O.; Cassee, F.; Hoek, G.; Fischer, P.; Brunekreef, B.; Krzyzanowski, M. Health effects of black carbon. In *WHO Regional Office for Europe*; WHO: Copenhagen, Denmark, 2012, pp 1−47.

(10) Han, Y. M.; Cao, J. J.; Lee, S. C.; Ho, K. F.; An, Z. S. Different characteristics of char and soot in the atmosphere and their ratio as an indicator for source identification in Xi'an, China. *Atmos. Chem. Phys.* **2010**, *10*, 595−607.

(11) Han, Y.; An, Z.; Marlon, J. R.; Bradley, R. S.; Zhan, C.; Arimoto, R.; Sun, Y.; Zhou, W.; Wu, F.; Wang, Q.; Burr, G. S.; Cao, J. Asian inland wildfires driven by glacial-interglacial climate change. *Proc. Natl. Acad. Sci. U.S.A.* **2020**, *117*, 5184−5189.

(12) Han, Y.; Cao, J.; Chow, J. C.; Watson, J. G.; An, Z.; Jin, Z.; Fung, K.; Liu, S. Evaluation of the thermal/optical reflectance method for discrimination between char- and soot-EC. *Chemosphere* **2007**, *69*, 569−574.

(13) Dusek, U.; Monaco, M.; Prokopiou, M.; Gongriep, F.; Hitzenberger, R.; Meijer, H. A. J.; Röckmann, T. Evaluation of a two-step thermal method for separating organic and elemental carbon for radiocarbon analysis. *Atmos. Meas. Tech.* **2014**, *7*, 1943−1955.

(14) Szidat, S.; Jenk, T. M.; Synal, H.-A.; Kalberer, M.; Wacker, L.; Hajdas, I.; Kasper-Giebl, A.; Baltensperger, U. Contributions of fossil fuel, biomass-burning, and biogenic emissions to carbonaceous aerosols in Zurich as traced by 14C. *J. Geophys. Res. Atmos.* **2006**, *111*, D07206.

(15) Zhang, Y. L.; Perron, N.; Ciobanu, V. G.; Zotter, P.; Minguillón, M. C.; Wacker, L.; Prévôt, A. S. H.; Baltensperger, U.; Szidat, S. On the isolation of OC and EC and the optimal strategy of radiocarbon-based source apportionment of carbonaceous aerosols. *Atmos. Chem. Phys.* **2012**, *12*, 10841−10856.

(16) Gustafsson, O.; Kruså, M.; Zencak, Z.; Sheesley, R. J.; Granat, L.; Engström, E.; Praveen, P. S.; Rao, P. S. P.; Leck, C.; Rodhe, H. Brown clouds over south Asia: Biomass or fossil fuel combustion? *Science* **2009**, *323*, 495−498.

(17) Dusek, U.; Hitzenberger, R.; Kasper-Giebl, A.; Kistler, M.; Meijer, H. A. J.; Szidat, S.; Wacker, L.; Holzinger, R.; Röckmann, T. Sources and formation mechanisms of carbonaceous aerosol at a regional background site in the Netherlands: insights from a year-long radiocarbon study. *Atmos. Chem. Phys.* **2017**, *17*, 3233−3251.

(18) Ni, H.; Huang, R.-J.; Cao, J.; Guo, J.; Deng, H.; Dusek, U. Sources and formation of carbonaceous aerosols in Xi'an, China: primary emissions and secondary formation constrained by radiocarbon. *Atmos. Chem. Phys.* **2019**, *19*, 15609−15628.

(19) Zhang, Y.-L.; Huang, R.-J.; El Haddad, I.; Ho, K.-F.; Cao, J.-J.; Han, Y.; Zotter, P.; Bozzetti, C.; Daellenbach, K. R.; Canonaco, F.; Slowik, J. G.; Salazar, G.; Schwikowski, M.; Schnelle-Kreis, J.; Abbaszade, G.; Zimmermann, R.; Baltensperger, U.; Prévôt, A. S. H.; Szidat, S. Fossil vs. non-fossil sources of fine carbonaceous aerosols in four Chinese cities during the extreme winter haze episode of 2013. *Atmos. Chem. Phys.* **2015**, *15*, 1299−1312.

(20) Jenk, T. M.; Szidat, S.; Schwikowski, M.; Gäggeler, H. W.; Brütsch, S.; Wacker, L.; Synal, H.-A.; Saurer, M. Radiocarbon analysis in an Alpine ice core: record of anthropogenic and biogenic contributions to carbonaceous aerosols in the past (1650-1940). *Atmos. Chem. Phys.* **2006**, *6*, 5381−5390.

(21) Yancheva, G.; Nowaczyk, N. R.; Mingram, J.; Dulski, P.; Schettler, G.; Negendank, J. F. W.; Liu, J.; Sigman, D. M.; Peterson, L. C.; Haug, G. H. Influence of the intertropical convergence zone on the East Asian monsoon. *Nature* **2007**, *445*, 74−77.

(22) Tylmann, W.; Fischer, H. W.; Enters, D.; Kinder, M.; Moska, P.; Ohlendorf, C.; Poręba, G.; Zolitschka, B. Reply to the comment by F. Gharbi on "Multiple dating of varved sediments from Lake Łazduny, northern Poland: Toward an improved chronology for the last 150 years". *Quat. Geochronol.* **2014**, *20*, 111−113.

(23) Han, Y. M.; Wei, C.; Huang, R.-J.; Bandowe, B. A. M.; Ho, S. S. H.; Cao, J. J.; Jin, Z. D.; Xu, B. Q.; Gao, S. P.; Tie, X. X.; An, Z. S.; Wilcke, W. Reconstruction of atmospheric soot history in inland regions from lake sediments over the past 150 years. *Sci. Rep.* **2016**, *6*, 19151.

(24) Dusek, U.; Cosijn, M. M.; Ni, H.; Huang, R.-J.; Meijer, H. A. J.; van Heuven, S. Technical note: An automated system for separate combustion of elemental and organic carbon for 14C analysis of carbonaceous aerosol. *Aerosol Air Qual. Res.* **2019**, *19*, 2604−2611.

(25) Ruff, M.; Wacker, L.; Gäggeler, H. W.; Suter, M.; Synal, H.-A.; Szidat, S. A gas ion source for radiocarbon measurements at 200 kV. *Radiocarbon* **2007**, *49*, 307−314.

(26) Synal, H.-A.; Stocker, M.; Suter, M. MICADAS: A new compact radiocarbon AMS system. *Nucl. Instrum. Methods Phys. Res., Sect. B* **2007**, *259*, 7−13.

(27) Reimer, P. J.; Brown, T. A.; Reimer, R. W. Discussion: Reporting and calibration of post-bomb C-14 data. *Radiocarbon* **2004**, *46*, 1299−1304.

(28) Wacker, L.; Bonani, G.; Friedrich, M.; Hajdas, I.; Kromer, B.; Němec, M.; Ruff, M.; Suter, M.; Synal, H.-A.; Vockenhuber, C. MICADAS: Routine and High-Precision Radiocarbon Dating. *Radiocarbon* **2010**, *52*, 252−262.

(29) Lan, J.; Wang, T.; Chawchai, S.; Cheng, P.; Zhou, K. e.; Yu, K.; Yan, D.; Wang, Y.; Zang, J.; Liu, Y.; Tan, L.; Ai, L.; Xu, H. Time marker of Cs-137 fallout maximum in lake sediments of Northwest China. *Quat. Sci. Rev.* **2020**, *241*, 106413.

(30) Wang, X.; Chu, G.; Sheng, M.; Zhang, S.; Li, J.; Chen, Y.; Tang, L.; Su, Y.; Pei, J.; Yang, Z. Millennial-scale Asian summer monsoon variations in South China since the last deglaciation. *Earth Planet. Sci. Lett.* **2016**, *451*, 22−30.

(31) Zhang, Y.-L.; Li, J.; Zhang, G.; Zotter, P.; Huang, R.-J.; Tang, J.-H.; Wacker, L.; Prévôt, A. S. H.; Szidat, S. Radiocarbon-Based Source Apportionment of Carbonaceous Aerosols at a Regional Background Site on Hainan Island, South China. *Environ. Sci. Technol.* **2014**, *48*, 2651−2659.

(32) Zhou, Y.; Xing, X.; Lang, J.; Chen, D.; Cheng, S.; Wei, L.; Wei, X.; Liu, C. A comprehensive biomass burning emission inventory with high spatial and temporal resolution in China. *Atmos. Chem. Phys.* **2017**, *17*, 2839−2864.

(33) Zhang, S. A review of the first national economic adjustment. *Contemporary China History Studies*; Contemporary Chinese History Research Editorial Department, 2008; Vol. *15*, pp 87−96.

(34) Wu, R.; Liu, F.; Tong, D.; Zheng, Y.; Lei, Y.; Hong, C.; Li, M.; Liu, J.; Zheng, B.; Bo, Y.; Chen, X.; Li, X.; Zhang, Q. Air quality and health benefits of China's emission control policies on coal-fired power plants during 2005-2020. *Environ. Res. Lett.* **2019**, *14*, 094016.

(35) Zhang, Q.; Zheng, Y.; Tong, D.; Shao, M.; Wang, S.; Zhang, Y.; Xu, X.; Wang, J.; He, H.; Liu, W.; Ding, Y.; Lei, Y.; Li, J.; Wang, Z.; Zhang, X.; Wang, Y.; Cheng, J.; Liu, Y.; Shi, Q.; Yan, L.; Geng, G.; Hong, C.; Li, M.; Liu, F.; Zheng, B.; Cao, J.; Ding, A.; Gao, J.; Fu, Q.; Huo, J.; Liu, B.; Liu, Z.; Yang, F.; He, K.; Hao, J. Drivers of improved PM2.5 air quality in China from 2013 to 2017. *Proc. Natl. Acad. Sci. U.S.A.* **2019**, *116*, 24463−24469.

(36) Tian, J.; Wang, Q.; Han, Y.; Ye, J.; Wang, P.; Pongpiachan, S.; Ni, H.; Zhou, Y.; Wang, M.; Zhao, Y.; Cao, J. Contributions of aerosol composition and sources to particulate optical properties in a southern coastal city of China. *Atmos. Res.* **2020**, *235*, 104744.

https://doi.org/10.1021/acs.est.1c05424
Environ. Sci. Technol. 2022, 56, 1534−1543

(37) An, Z.; Huang, R.-J.; Zhang, R.; Tie, X.; Li, G.; Cao, J.; Zhou, W.; Shi, Z.; Han, Y.; Gu, Z.; Ji, Y. Severe haze in northern China: A synergy of anthropogenic emissions and atmospheric processes. *Proc. Natl. Acad. Sci. U.S.A.* **2019**, *116*, 8657−8666.
(38) Junker, C.; Liousse, C. A global emission inventory of carbonaceous aerosol from historic records of fossil fuel and biofuel consumption for the period 1860-1997. *Atmos. Chem. Phys.* **2008**, *8*, 1195−1207.
(39) Wang, R.; Tao, S.; Wang, W.; Liu, J.; Shen, H.; Shen, G.; Wang, B.; Liu, X.; Li, W.; Huang, Y.; Zhang, Y.; Lu, Y.; Chen, H.; Chen, Y.; Wang, C.; Zhu, D.; Wang, X.; Li, B.; Liu, W.; Ma, J. Black Carbon Emissions in China from 1949 to 2050. *Environ. Sci. Technol.* **2012**, *46*, 7595−7603.
(40) Bond, T. C.; Sun, H. Can reducing black carbon emissions counteract global warming? *Environ. Sci. Technol.* **2005**, *39*, 5921−5926.
(41) Steffen, W.; Broadgate, W.; Deutsch, L.; Gaffney, O.; Ludwig, C. The trajectory of the Anthropocene: The Great Acceleration. *Anthr. Rev.* **2015**, *2*, 81−98.
(42) Zalasiewicz, J.; Waters, C. N.; Williams, M.; Barnosky, A. D.; Cearreta, A.; Crutzen, P.; Ellis, E.; Ellis, M. A.; Fairchild, I. J.; Grinevald, J.; Haff, P. K.; Hajdas, I.; Leinfelder, R.; McNeill, J.; Odada, E. O.; Poirier, C.; Richter, D.; Steffen, W.; Summerhayes, C.; Syvitski, J. P. M.; Vidas, D.; Wagreich, M.; Wing, S. L.; Wolfe, A. P.; An, Z.; Oreskes, N. When did the Anthropocene begin? A mid-twentieth century boundary level is stratigraphically optimal. *Quat. Int.* **2015**, *383*, 196−203.
(43) Lu, Y.; Teng, Z. *General History of Chinese Population*; The Peoples Press of Shandong: Jinan: China, 2000; pp 645−1183.
(44) China-Automobile-Industry-History-Editorial-Committee. *History of China's Automobile Industry: 1901−1990*; People's Communications Press: Beijing, China, 1996; pp 1−315.
(45) Compilation-Team-of-Modern-Coal-Mine-History-of-China. *Modern Coal Mine History of China*; Coal Industry Press: Beijing, China, 1990; pp 1−545.
(46) Zhao, D. *Modern Economic History of China*; High Education Press: Beijing, China, 2016; pp 1−356.

https://doi.org/10.1021/acs.est.1c05424
Environ. Sci. Technol. 2022, 56, 1534−1543